



Fermi National Accelerator Laboratory

FERMILAB-Conf-95/303-E

D0

Top Physics at D0

B. Klima

For the D0 Collaboration

*Fermi National Accelerator Laboratory
P.O. Box 500, Batavia, Illinois 60510*

September 1995

Presented at the *17th International Symposium on Lepton-Photon Interactions*,
Beijing, China, August 10-15, 1995

Disclaimer

This report was prepared as an account of work sponsored by an agency of the United States Government. Neither the United States Government nor any agency thereof, nor any of their employees, makes any warranty, expressed or implied, or assumes any legal liability or responsibility for the accuracy, completeness, or usefulness of any information, apparatus, product, or process disclosed, or represents that its use would not infringe privately owned rights. Reference herein to any specific commercial product, process, or service by trade name, trademark, manufacturer, or otherwise, does not necessarily constitute or imply its endorsement, recommendation, or favoring by the United States Government or any agency thereof. The views and opinions of authors expressed herein do not necessarily state or reflect those of the United States Government or any agency thereof.

Top Physics at DØ

BOAZ KLIMA

Fermilab

Batavia, IL 60510, USA

E-mail: klima@fnal.fnal.gov

for

the DØ Collaboration

ABSTRACT

The DØ collaboration reports on the observation of the Standard Model top quark in $p\bar{p}$ collisions at $\sqrt{s} = 1.8$ TeV at the Fermilab Tevatron. We have searched for $t\bar{t}$ production with an integrated luminosity of approximately 50 pb^{-1} in the dilepton and single-lepton decay channels, with and without tagging of b quark jets. We observe 17 events with an expected background of 3.8 ± 0.6 events. The probability for an upward fluctuation of the background to produce the observed signal is 2×10^{-6} (equivalent to 4.6 standard deviations). The kinematic properties of the excess events are consistent with top quark decay. We measure the top quark mass to be 199^{+19}_{-21} (stat.) $^{+14}_{-21}$ (syst.) GeV/c² and its production cross section to be 6.4 ± 2.2 pb. DØ also sees a hadronic W mass peak ($W \rightarrow jj$) in the $t\bar{t}$ data events. Preliminary results from multivariate analyses and from the $t\bar{t} \rightarrow \text{all-jets}$ channel are discussed. Preliminary determination of the top quark mass using dilepton events yields 145 ± 25 (stat.) ± 20 (syst.) GeV/c².

1. Introduction

The Standard Model requires that the b quark have a weak isospin partner, the top quark. The search for the top quark and the measurement of its properties are an important test of the Standard Model. Certain Standard Model parameters, including m_W , m_Z , $\sin^2 \theta_W$, and Z boson decay asymmetries depend on the top quark mass, and to a lesser extent on the Higgs boson mass, through radiative corrections involving top quark loops. Precision measurements of these parameters permit an indirect measurement of the top quark mass which can be compared to that obtained by direct measurement. These precision measurements currently suggest a top quark mass in the range 150–210 GeV/c², depending on the Higgs mass¹.

Direct searches for the Standard Model top quark have been carried out at the Fermilab Tevatron by the DØ and CDF experiments. Earlier results from these experiments based on data from the 1992–1993 Tevatron run include a lower limit on the top quark mass, m_t , of 131 GeV/c² by DØ², a 2.8 standard deviation (σ) positive result by CDF³, and a 1.9σ positive result by DØ⁴.

In this article, we report on the DØ discovery of the top quark (section 2), and the

measurement of its mass using single-lepton events⁵ (section 3). The CDF concurrent discovery is described elsewhere⁶. We also show that our top data sample contains W 's which decay hadronically (section 4), and we report preliminary results from multivariate analyses (section 5) and from the $t\bar{t} \rightarrow \text{all-jets}$ channel (section 6). Finally, we present a preliminary measurement of the top quark mass using dilepton events (section 7).

2. The Discovery of the Top Quark

The DØ detector, its data collection systems and particle identification definitions are described elsewhere^{7,8,9}. Data used for the analysis were collected during the 1992-1993 and 1994-1995 Tevatron runs, with an integrated luminosity of about 50pb^{-1} but with slight differences among the decay channels. In the analysis we assume that the top quark is pair-produced and decays 100% of the time into a W boson and a b quark. The search is divided into seven independent channels depending on how the two W bosons decay, and on whether or not a soft muon from a b or c quark semileptonic decay is observed. The so-called dilepton channels occur when both W bosons decay leptonically ($e\mu + \text{jets}$, $ee + \text{jets}$, and $\mu\mu + \text{jets}$). The single-lepton channels occur when just one W boson decays leptonically ($e + \text{jets}$ and $\mu + \text{jets}$). The single-lepton channels are subdivided into b -tagged and untagged channels according to whether or not a muon consistent with $b \rightarrow \mu + X$ is observed. The muon-tagged channels are denoted $e + \text{jets}/\mu$ and $\mu + \text{jets}/\mu$.

The event selection for this analysis is chosen to optimise expected significance for top quark masses of 180–200 GeV/ c^2 , using the ISAJET event generator¹⁰ to model the top quark signal (assuming the calculated Standard Model top quark pair production cross section¹¹), and using our standard background estimates^{5,8}. In this analysis, we achieve an expected signal-to-background ratio of 1:1 for a top quark mass of 200 GeV/ c^2 . This is a better signal-to-background ratio, but with smaller acceptance, than our previously published analyses^{2,4}. The improved rejection arises primarily by requiring events to have a larger total transverse energy by means of a cut on a quantity we call H_T . H_T is defined as the scalar sum of the E_T 's of the jets (for the single-lepton and $\mu\mu + \text{jets}$ channels, or the scalar sum of the E_T 's of the leading electron and the jets (for the $e\mu + \text{jets}$ and $ee + \text{jets}$ channels). In addition to the “standard” event selection, a “loose” selection is defined which does not include an H_T cut. This is done as a consistency check and to provide a less biased event sample for the top quark mass analysis.

The signature for the dilepton channels is two isolated leptons, two or more jets, and large \cancel{E}_T . The signature for the single-lepton channels is one isolated lepton, large \cancel{E}_T , and three or more jets (with muon tag) or four or more jets (without tag). The single-lepton signature includes either a soft muon tag or a “topological tag,” based on H_T and the aplanarity of the jets \mathcal{A} , which is proportional to the smallest

Table 1: Summary of number of events observed, the predicted background, and the probability for the background to account for the data for both standard and loose cuts. A $t\bar{t}$ production cross section ($\sigma_{t\bar{t}}$) is also given for $m_t = 200$ GeV/ c^2 .

	Standard Selection	Loose Selection
Dileptons	3	4
Lepton + Jets (Shape)	8	23
Lepton + Jets (Muon tag)	6	6
All channels	17	33
Background	3.8 ± 0.6	20.6 ± 3.2
Probability	2×10^{-6} (4.6σ)	0.023 (2.0σ)
$\sigma_{t\bar{t}}$ ($m_t = 200$ GeV/ c^2)	6.3 ± 2.2 pb	4.5 ± 2.5 pb

eigenvalue of the momentum tensor of the jets in the laboratory frame. “Double-tagged” events are counted only once, contributing to the muon tagged channels. A detailed summary of the kinematic cuts, both “standard cuts” and “loose cuts”, can be found elsewhere^{5,8,9}. The loose event selection cuts differ from the standard ones by the removal of the H_T requirement and by the relaxation of the aplanarity requirement for $e + \text{jets}$ and $\mu + \text{jets}$.

The acceptance for $t\bar{t}$ events is calculated using the ISAJET event generator¹⁰ and a detector simulation based on the GEANT program¹³. Differences in the acceptance found using the HERWIG event generator¹⁴ are included in the systematic error. Physics backgrounds (those having the same final state particles as the signal) were estimated using Monte Carlo (MC) simulation or a combination of Monte Carlo and data. The instrumental background from jets misidentified as electrons is estimated entirely from data using the measured jet misidentification probability (typically 2×10^{-4}). Other backgrounds for muons (*e.g.* hadronic punchthrough and cosmic rays) are found to be negligible for the signatures in question.

From all seven channels, we observe 17 events with an expected background of 3.8 ± 0.6 events (see Table 1). Our measured cross section ($\sigma_{t\bar{t}}$) as a function of the top quark mass hypothesis is shown in Fig. 1. The variation in $\sigma_{t\bar{t}}$ is due to the dependence of the efficiency on m_t . Assuming a top quark mass of 200 GeV/ c^2 , the production cross section is 6.3 ± 2.2 pb. The error in the cross section includes an overall 12% uncertainty in the luminosity. The probability of an upward fluctuation of the background to 17 or more events is 2×10^{-6} , which corresponds to 4.6 standard deviations for a Gaussian probability distribution. We have calculated the probability for our observed distribution of excess events among the seven channels and find that our results are consistent with top quark branching fractions at the 53% CL. A top production cross-section was calculated for the dilepton, tagged, and untagged single-lepton channels independently assuming the top hypothesis both for the “standard cuts” and “loose cuts”. All agree within the errors as shown in Fig. 2. Thus, we

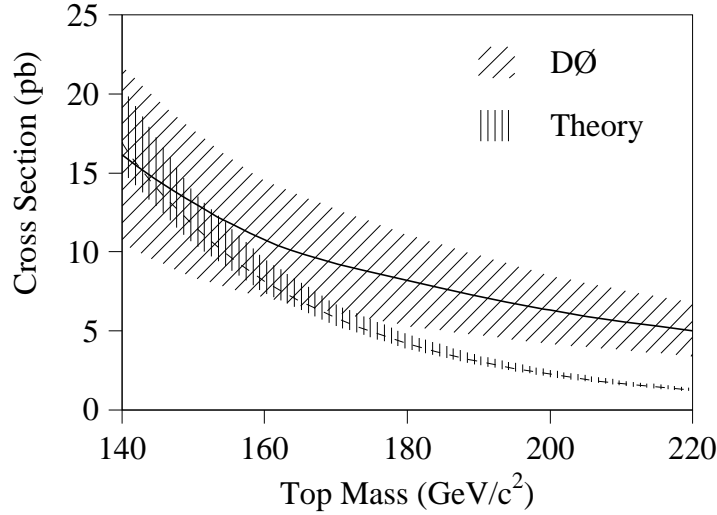


Figure 1: DØ measured $t\bar{t}$ production cross section (solid line with one standard deviation error band) as a function of assumed top quark mass. Also shown is the theoretical cross section¹¹ curve (dashed line).

observe a statistically significant excess of events, and the distribution of events among the seven channels is consistent with top quark production. We conclude that we have observed the top quark.

3. The Lepton+jets Mass Analysis

We can extract the top quark mass from our single-lepton + ≥ 4 jets event sample using a two-constraint (2C) kinematic fit to the hypothesis $t\bar{t} \rightarrow W^+W^-b\bar{b} \rightarrow \ell\nu q\bar{q}b\bar{b}$. Assignment of the four highest E_T jets (using a $\mathcal{R} = 0.3$ cone algorithm) to partons is made using all combinations of jet assignments consistent with tagged b jets. The measured jet energy inside the jet cone is corrected to the energy of the original parton. We test our jet energy corrections by examining the E_T balance in $Z(\rightarrow ee) + \text{jets}$ data events.

The degree of ambiguity in the mass-fitting problem is larger than suggested by naive combinatoric analysis. Effects such as gluon radiation and jets being lost due to merging or falling below energy thresholds make the correct solution more difficult, and sometimes impossible, to find. In cases where there are more than four jets, we use only the four highest E_T jets. Rather than simply using the solution with the smallest χ^2 , we use a χ^2 -probability-weighted average top quark mass (with weight $e^{-\chi^2/2}$) from up to three solutions having $\chi^2 < 7$. The top quark mass resolution obtained in this way is found to be slightly better than that which is obtained from the smallest χ^2 solution alone. The effects of wrong combinations, initial state gluon radiation (ISR),

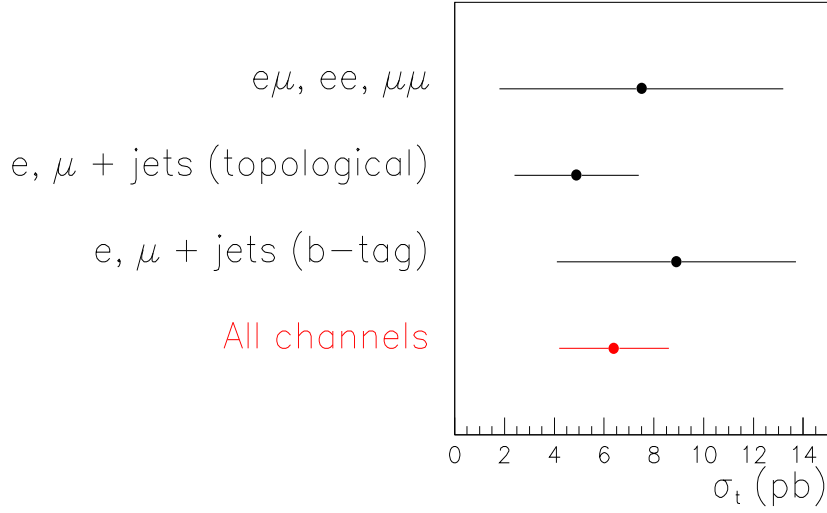


Figure 2: DØ measured $t\bar{t}$ production cross section (at $m_t = 200 \text{ GeV}/c^2$) using dilepton events, using single-lepton with “topological tag” events, using single-lepton with “soft μ tag” events, and using events from all channels.

and final state gluon radiation (FSR) on the top quark mass resolution are taken into account using MC data samples with different m_t . These MC samples yield a family of distributions in fitted top mass as a function of the input top mass. A similar distribution of fitted mass is determined for the background processes.

An unbinned maximum likelihood fit is used to extract the top quark mass likelihood distribution from a given sample of candidate events. The likelihood function used is given by:

$$L = e^{-(n_b - \langle n_b \rangle)^2 / 2\sigma^2} \frac{(n_s + n_b)^N}{N!} e^{-(n_s + n_b)} \prod_i \frac{n_s f_s(m_t, m_i) + n_b f_b(m_i)}{n_s + n_b} \quad (1)$$

The unknowns are the number of expected signal events n_s , the number of expected backgrounds n_b , and the top quark mass m_t . The inputs are the number of candidate events N , the fitted masses of the candidate events $m_i, (i = 1, \dots, N)$, and the nominal background $\langle n_b \rangle$ and its error σ as determined in the counting experiment. The functions f_s and f_b are the expected distributions of fitted mass for signal and background. The likelihood function consists of three multiplicative factors representing the constraints on the background normalization, overall Poisson counting statistics, and the relative likelihood for each event to be a top quark event (for a given top quark mass) or background.

The entire mass determination machinery has been tested using MC data. We have verified that mass bias of the kinematic fit is removed by the likelihood fit, and that the statistical error on the top quark mass from the likelihood fit scales inversely

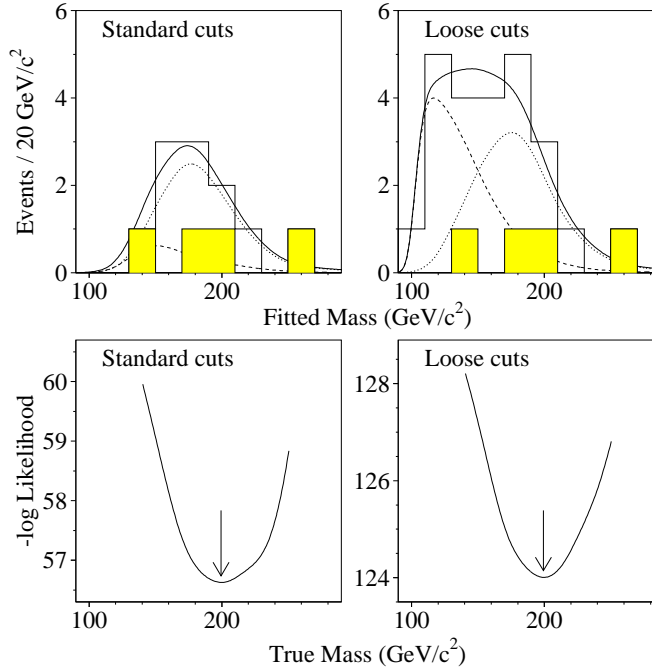


Figure 3: Fitted mass and mass likelihood distributions for candidate events (histogram; shaded - μ tag) with the expected distribution for top (dotted curve), background (dashed), and top + background (solid) for standard and loose cuts.

as the square root of the number of candidate events.

Eleven of the 14 single-lepton + ≥ 4 jets candidate events selected using the standard cuts, and 24 of the 29 candidate events selected using the loose cuts, have successful kinematic fits. The kinematic fit can fail because there are fewer than four jets (in the case of b -tagged events), or because there are no solutions with good χ^2 . The fitted mass and likelihood distributions of these events are shown in Fig. 3.

The top quark mass extracted from the likelihood curve is 199_{-25}^{+31} (stat.) GeV/c^2 for standard cuts and 199_{-21}^{+19} (stat.) GeV/c^2 for loose cuts. The statistical errors are derived using $\Delta \ln(L) = 0.5$. The result of the likelihood fit for the loose cuts sample does not change significantly if the background constraint is removed from the likelihood function, thus confirming the prior estimate of the background level. Because of its smaller error and reduced sensitivity to a-priori background estimates, we use the loose cuts mass determination as our preferred mass result.

The systematic error on the mass determination is dominated by the jet energy scale uncertainty which we estimate conservatively to be 10%. The top mass measurement depends on having an event generator that realistically models effects such as gluon radiation and jet shapes. Our result above is based on ISAJET; repeating the analysis using HERWIG results in a 4 GeV/c^2 lower mass which we include in the systematic error. The total systematic error on the top quark mass is $_{-21}^{+14}$ GeV/c^2 .

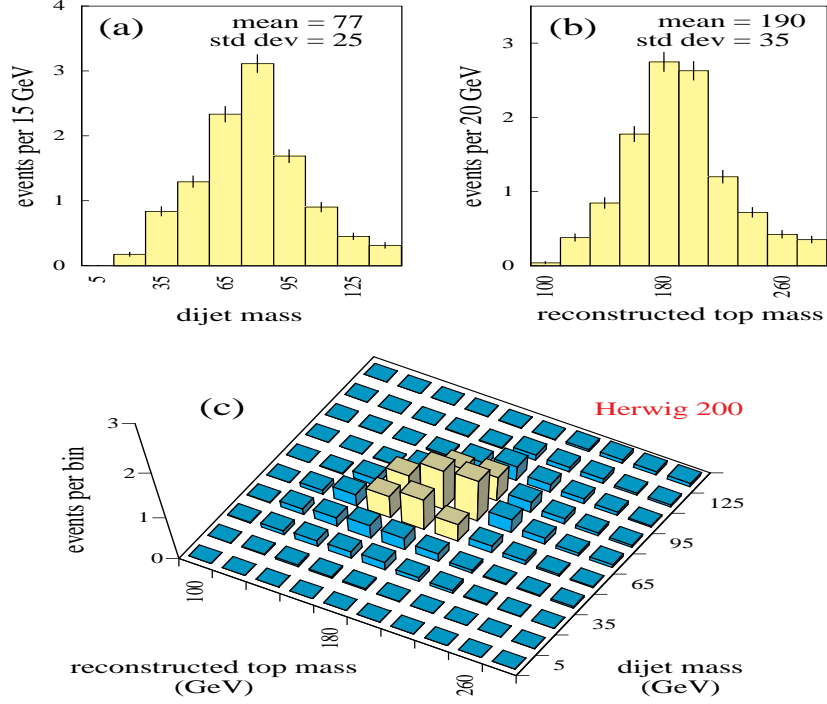


Figure 4: (a,b) Projections and (c) 2-dim plot of HERWIG 200 GeV/c² top MC events *vs.* reconstructed top mass and dijet mass.

We measure the top quark pair production cross section at our central top quark mass to be $\sigma_{t\bar{t}} = 6.4 \pm 2.2$ pb.

4. $W \rightarrow jj$ in $t\bar{t}$ data events

The statistical significance of the DØ top quark signal is established by its published⁵ counting experiment, in which we also displayed a clear excess of events having large trijet mass and minimum dijet mass compared to expected background. The “loose” cut 2C top quark mass analysis, reviewed in section 3, obtains a top mass lineshape which is different from that of expected background. As just noted, the top quark mass determined in the 2C likelihood analysis is essentially unchanged if the constraint on background normalization is removed. This supports the background calculation used by the counting experiment.

These points having been established, we re-examine the reconstructed top and dijet masses in the single-lepton data events to give independent confirmation that the top quark does decay to W boson decaying hadronically ($W \rightarrow jj$).

Since no $m_{jj} - m_W$ constraint should be applied in a study of the dijet mass, the kinematic fits now have only 4 (8) distinct pairs $m(bl\nu)$, $m(bjj)$ when a soft

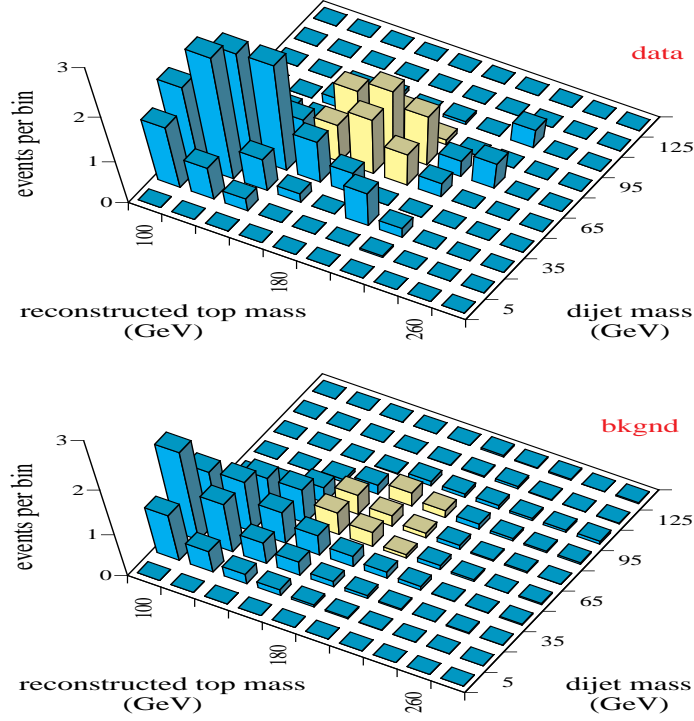


Figure 5: 2-dim distributions in reconstructed top mass and dijet mass of (a) $D\bar{O}$ data, and (b) background.

μ tag is (is not) present. Half of these involve the larger of two possible neutrino longitudinal momenta. These solutions are less likely than their complements and are rejected. The remaining two or four solutions are weighted according to $e^{-\chi^2/2}$ with $\chi^2 \propto \ln^2(m(bl\nu)/m(bjj))$. The weight for each event is normalized to unity.

For the reconstructed top quark mass m_t we plot the weighted average of $m(bl\nu)$ and $m(bjj)$. For the dijet mass m_{jj} , when the b jet from $t \rightarrow bjj$ is untagged, we typically assign the b to jet 1 (the most energetic in the top CM) and correspondingly plot m_{23} and m_{13} with equal weight. We emphasize that dijet energies are not varied, and dijets are not selected for consistency with m_W . When applied to 200 GeV/ c^2 HERWIG top quark MC, this analysis method yields the two dimensional plot and its projections shown in Fig. 4. A clear peak in both reconstructed top and dijet mass is evident. The reconstructed top and dijet mass peaks are close to the true top and W masses, respectively. The peak widths scale roughly as \sqrt{m} . Varying the true top mass does not substantially move the mass at which the dijet peak occurs, but the wings of the dijet distribution do change.

When applied to the appropriate combination of backgrounds, the same analysis yields the quite different plot in Fig. 5(b). Most event weights populate quite small m_t and m_{jj} . Figure 5(a) presents the plot of the data. Figure 6 displays projections on

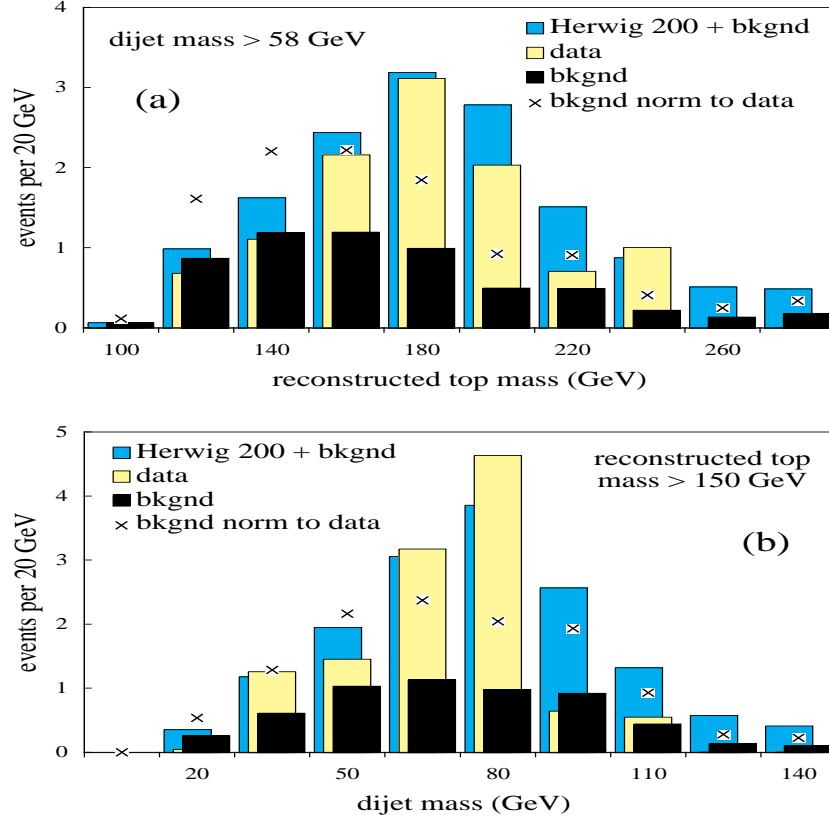


Figure 6: Distributions of (a) reconstructed top mass m_t and (b) dijet mass m_{jj} with (a) $m_{jj} > 58 \text{ GeV}/c^2$ and (b) $m_t > 150 \text{ GeV}/c^2$ for (light dashed) $D\bar{O}$ data, (medium) sum of background and HERWIG 200 GeV/c^2 top MC, (black) background alone, and (X's) background normalized to match the area of the data.

the reconstructed top and dijet mass axes of the data. Here we avoid the domination of background in the projections by plotting dijet masses only for reconstructed top masses exceeding $150 \text{ GeV}/c^2$, and by plotting reconstructed top masses only for dijet masses exceeding $58 \text{ GeV}/c^2$. Shown for comparison are the same projections for the expected combination of signal and background, and for background alone.

We interpret the reconstructed top mass projection in Fig. 6(a) as evidence for a top quark mass peak. The data are distributed in the shape of a peak, in agreement with expectation. In contrast the background is smaller in magnitude relative to the expected component; it is shifted and dissimilar in shape. Likewise, we interpret the dijet mass projection in Fig 6(b) as evidence for a W mass peak. Again, the data are peaked, as is the expected combination of signal and background, the background is smaller in magnitude than for $t\bar{t}$, and it is much broader in shape. Figure 5(a) confirms that the top and W peaks indeed arise mainly from the same events. The

data are very different from the background (Fig. 5(b)).

5. Multivariate Analyses

In the previous analyses, conventional methods were used to optimize independent cuts on kinematic variables. However, these techniques do not exploit correlations among the cut variables and thus may cause a loss in signal efficiency. Recently we have applied the multivariate methods of the Probability Density Estimation (PDE) and the Neural Network (NN) for identifying top quark events and improving the signal efficiency^{16,15}. We use the PDE and the NN methods to analyze e +jets data corresponding to an integrated luminosity of about 50pb^{-1} . To achieve higher signal efficiency than for our conventional analysis, we relax the number of jets required and carry out an analysis of the $e+ \geq 3$ jets data. The on-line trigger selection, off-line electron and muon identification criteria and description of variables used can be found elsewhere^{8,9}.

In the PDE analysis¹⁵ the pre-selection criteria are $E_T^e > 20$ GeV/c, $\cancel{E}_T > 20$ GeV/c and at least 3 jets with $E_T > 15$ GeV/c. These five transverse energies define our input vector in the analysis. The two backgrounds are combined in the ratio estimated as in the conventional analysis and are treated as a single background for building the probability density functions. Figure 7 shows the distributions of the discriminant function, D , for background events, $180\text{ GeV}/c^2$ MC top quark events ($t\bar{t}180$) and for $D\bar{O}$ data. Applying a cut of $D > 0.8$ yields 21 data events with an estimated background of 14.0 ± 1.6 events. The product of efficiency and branching ratio for $t\bar{t}180$ events is 3.1% (as compared to 1.8% for conventional analysis). The $t\bar{t}$ cross-section is calculated to be 4.7 ± 3.3 (stat.) pb , in agreement with the results from the conventional analysis.

The NN analyses of the $e+ \geq 4$ jets data with two and six variables have been discussed previously¹⁶. Here we present results from a five-variable analysis. The NN program used here is JETNET 3.0¹⁸. We use E_T^e, \cancel{E}_T, E_T of jets in the event, the event shape variable aplanarity (\mathcal{A}) and the total transverse energy H_T of central jets to discriminate the top signal events from the backgrounds. We use a five-dimensional input vector $x = (E_T^e, \cancel{E}_T, H_T, \mathcal{A}, E_T^{jet3})$. For this analysis, we use two different networks to discriminate against W +jets and QCD fake background separately. We use networks with 5 input nodes, 5 hidden nodes in one hidden layer and one output node. The target output of the network during training is set to be 1 for the signal and 0 for the background.

Figures 8(a)-8(d) show the output of the first network (NN1) for $t\bar{t}180$, W +jets, QCD fakes and for $D\bar{O}$ data. The distributions peak close to 1 for signal events and close to 0 for background events, as expected. To get better rejection of QCD fakes, we process all samples through the second network. In Figs. 8(e)-8(h) we show the output of the second network (NN2) for signal, background and data events which

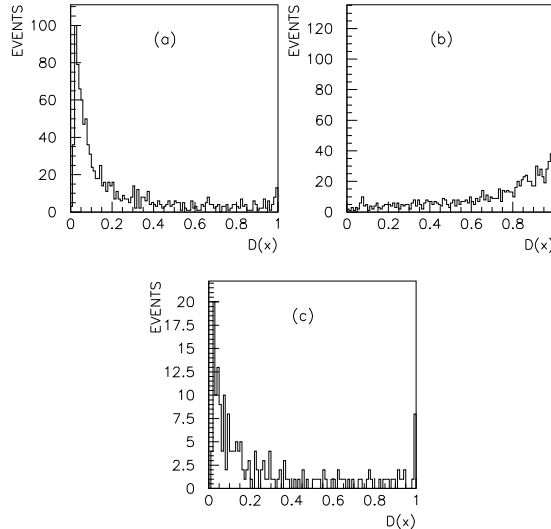


Figure 7: The PDE discriminant function for (a) background, (b) 180 GeV/c² MC top quark events and (c) DØ data.

satisfy the cut $NN1 > 0.7$.

Applying the cuts $NN1 > 0.7$ and $NN2 > 0.5$ yields 25 candidate events with an estimated background of 10.1 ± 1.5 . This gives an excess over background of 14.9 ± 5.2 events. The 25 candidate events found here include most of the non-tagged and μ -tagged candidate events found by the conventional analysis. The product of efficiency and branching ratios is 4.0% (compared to 1.8 % for conventional analysis) for $t\bar{t}180$. For a top quark mass of 200 GeV/c², we obtain a $t\bar{t}$ production cross-section of 6.7 ± 2.3 pb (stat.). A preliminary estimate of the systematic uncertainty which includes errors in background estimation and signal efficiency (prior to multivariate analyses) and NN specific uncertainties is about 30%. This is dominated by the first two components and work is in progress to reduce these uncertainties.

6. The $t\bar{t} \rightarrow \text{all-jets}$ Channel

In the Standard Model, the dominant decay channel for top quarks is a b quark and a W boson, with the W boson decaying into a quark-antiquark pair. The $t\bar{t}$ events with both W 's decaying hadronically are referred to as the “all-jets” channel and account for 44% of the $t\bar{t}$ production.

The signature for $t\bar{t}$ production in the all-jets channel is six (or more) high momentum jets, with kinematic properties consistent with a $t\bar{t}$ decay hypothesis. The background for this signature is predominantly QCD multijet production. The search for the top quark in the all-jets channel begins with the imposition of preliminary selection criteria at the trigger stage and in the offline analysis. These include 6 or more central jets with cone size $\mathcal{R} = 0.3$, no isolated electron or muon, and high H_T .

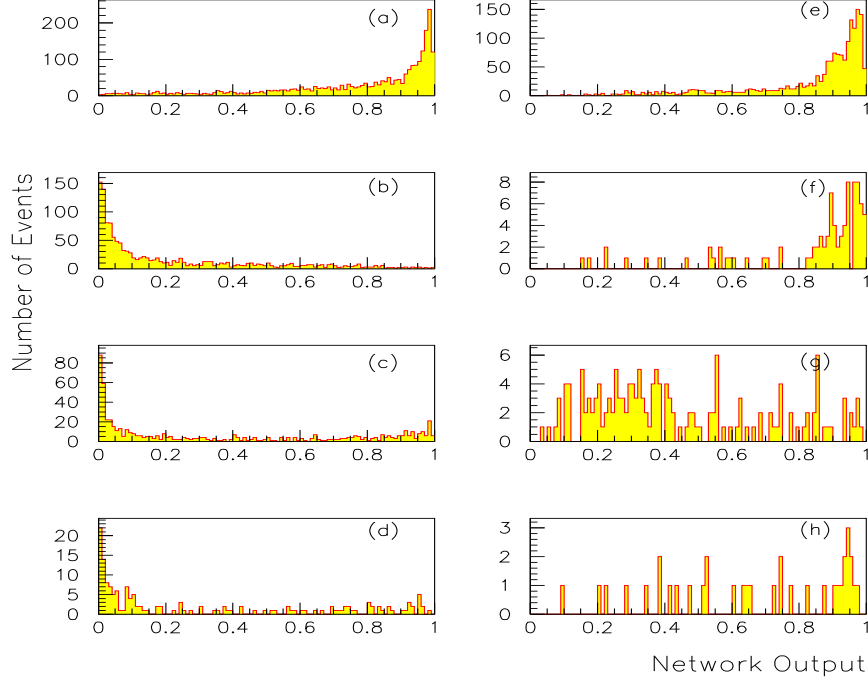


Figure 8: Distributions of the output from the first network for (a) $t\bar{t}$ 180, (b) W +jets (VECBOS), (c)QCD fakes and (d) $D\bar{D}$ data, and distributions of the output from the second network for (e) $t\bar{t}$ 180, (f) W +jets (VECBOS), (g)QCD fakes and (h) $D\bar{D}$ data,

These criteria are not very restrictive, and the observed cross section is more than one thousand times larger than the expected signal. The principal challenge in this search is to develop a set of selection criteria that can significantly improve the signal to background ratio and provide an estimate of the remaining background.

In addition to the initial selection, we use the following four kinematic parameters: the scalar sum of jet E_T excluding the two leading jets (H_T^{3j}), the aplanarity (\mathcal{A}), the centrality (\mathcal{C}) of the event given by the ratio of H_T to H_E , where H_E is the sum of jet energies, and the averaged number of jets (N_j^{Ave}), defined as the number of jets averaged over a range of E_T thresholds, weighted by the E_T threshold.

After applying cuts based on the above parameters, we require a soft muon to tag the b -jets. Because every $t\bar{t}$ event contains two high- E_T b -quark jets, this requirement enriches the $t\bar{t}$ component of the sample, roughly by an order of magnitude.

Due to a lack of reliable MC sample for background processes, a significant fraction of the data sample is used to model background properties, and the search for signal is concentrated on the rest of the data sample. This ensures that the criteria are derived from an event sample that is statistically independent of the data used in the search.

Selection criteria	No. Data events	$N_{t\bar{t}}$ ($m_t=200$ GeV/c ²)	N_{bkg} μ -tag	observed μ -tag	expected $t\bar{t}$ μ -tag
none	58327	104.1	1017.5	1053	22.1
loose	1459	48.2	40.8	50	10.4
medium	369	25.5	11.6	13	5.4
tight	66	9.8	2.3	4	2.3

Table 2: Comparison of number of μ -tagged events in Run Ib with expected background and $t\bar{t}$ signal. The number of $t\bar{t}$ events includes contributions from other top quark decay channels that pass the selection criteria.

Muon-tagging in the all-jets channel is done in the same way as the lepton+jets channel. Muon tagging can achieve additional background rejection but with a substantial loss of potential signal. This loss in efficiency is acceptable because μ -tagging permits a straightforward and reliable estimate of the background expected in a data sample. The background tag rate is parameterized as a function of jet E_T , and the tag rate function is applied to the candidate sample of events to estimate the background. For three sets of selection cuts, the number of predicted signal (using ISAJET 200 GeV/c² $t\bar{t}$ MC), the expected background, and the number of observed data events is shown in Table 2. Indication of a small excess is observed.

Preliminary results from double-tag events, those in which one finds two soft μ 's, are also obtained. Two sets of selection cuts, “tight” and “loose”, are examined. These sets of cuts are different from the ones used in the single-tag analysis. With the “tight” (“loose”) cuts the expected number of background events is 1.0 (60.1), while the number of observed data events is 3 (69). The statistical errors on the background events are very small due to the large data set. The systematic errors, however, are expected to be larger; this study is incomplete. Nevertheless, the preliminary results show evidence for a small excess.

7. The Dilepton Mass Analysis

In this section we describe a measurement of the mass of the top quark based on dilepton events. We define an algorithm that returns a single number as the top mass estimator for every dilepton event¹⁹. We then calibrate the relationship of this variable to the top quark mass using a MC simulation. From the simulation we obtain its spectrum as a function of the top quark mass. A maximum likelihood fit of the MC spectra to the spectrum observed in the data then gives the value of the top quark mass that best fits the data.

There are two neutrinos in a dilepton event, one from each top quark. Therefore neither top quark can be reconstructed directly and we have to resort to an indirect estimate of the top quark mass. A dilepton event is completely defined by 18 numbers: the components of the momentum vectors of the six final state particles. We measure

14 of them directly and can impose four constraints on the invariant mass of the decay products of the W bosons and the top quarks. Thus, for each assumed value m_t of the top mass we can solve for the four unmeasured final state momentum components. There may be 0, 2, or 4 solutions which are consistent with the observed final state. References^{19,20} describe in detail how the solutions are found.

Due to gluon radiation there may be more than two jets in dilepton events. In the absence of b jet identification, we assume that the b jets are the two highest E_T jets in the event and ignore all other jets. This assignment is correct for 53% of the events for $m_t = 140 \text{ GeV}/c^2$. Since we cannot distinguish between particles and antiparticles we are left with a two-fold ambiguity in assigning the leptons and jets to the two top quark decays, which doubles the number of possible solutions to eight.

Not all solutions are equally likely and we assign a weight to each solution^{19,20}, which includes the proton structure function for valence quarks, and the probability density function for the energy of the charged lepton in the rest frame of the top quark.

Due to detector resolutions, the observed momenta are not equal to the true momenta of the final state particles. We therefore integrate the weight over all final states that are consistent with the observed event. We approximate this by averaging the weight over final states with momenta which are distributed normally around the observed values with standard deviations equal to the detector resolutions.

In order to account for initial and final state gluon radiation and the resulting jet combinatorics, we calibrate the weight function with a MC model that contains these effects. We choose the value of m_t at which the weight function assumes its maximum, m_{peak} , as the estimator for the top quark mass.

To extract a measurement of the top quark mass from a sample of dilepton events, we perform a maximum likelihood fit to the distribution of the observed mass in the data. This procedure is similar to that in the lepton+jets mass analysis (section 3).

The event selection criteria are the same as for the cross section analysis⁵. In a data sample corresponding to $\approx 72 \text{ pb}^{-1}$, five dilepton candidate events were found (1 ee , 2 $e\mu$, and 2 $\mu\mu$). Figure 9(a) shows the resolution function for the fitted mass and the m_{peak} values of the 5 events. The result of the maximum likelihood fit is $m_{fit} = 144 \pm 17 \text{ GeV}/c^2$ for all five events and $m_{fit} = 145 \pm 22 \text{ GeV}/c^2$ for the two $e\mu$ events only. The likelihood function for all five events is shown in Fig. 9(b). The statistical errors are derived using $\Delta \ln(L) = 0.5$. Since the rms of fits for ensembles of five MC event experiments is larger ($25 \text{ GeV}/c^2$ at $m_t \approx 145 \text{ GeV}/c^2$), we use this as our preliminary estimate of the statistical error. Systematic errors are due to jet energy scale, parametrization of the resolution functions, different MC generators, and uncertainty in the signal to background ratio. Fitting with no background in the resolution function changes the result to $148 \text{ GeV}/c^2$ while fitting with ≈ 3 times the estimated background changes it to $140 \text{ GeV}/c^2$, leading to an error of $4 \text{ GeV}/c^2$.

Our preliminary measured top quark mass using the five dilepton candidates is

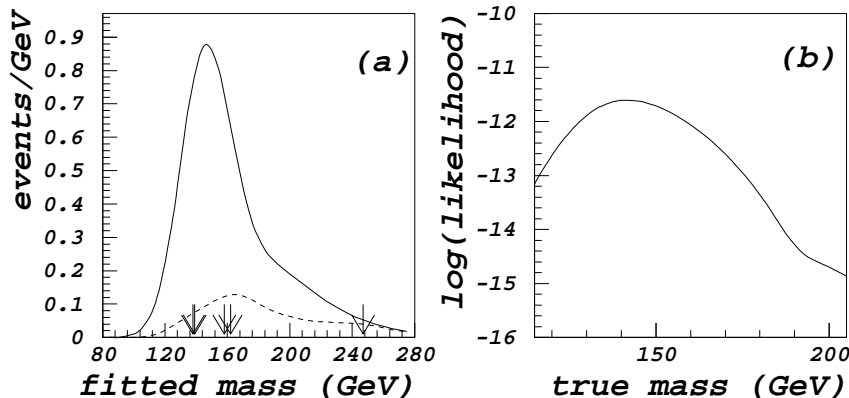


Figure 9: (a) Expected contributions from signal with $m_{top} = 144 \text{ GeV}/c^2$ (solid) and background (dashed) to the resolution function. The arrows indicate the peak positions of the weight functions for the five dilepton events. (b) Likelihood function for these events with parabolic fit.

$$m_{top} \approx 145 \pm 25(\text{stat}) \pm 20(\text{syst}) \text{ GeV}/c^2.$$

8. Conclusions

We have searched for top quark signals in seven channels in a data sample having an integrated luminosity of 50 pb^{-1} . We observe 17 candidate events with an expected background of 3.8 ± 0.6 events. The excess is statistically significant. The probability for the background to fluctuate up to 17 events is 2×10^{-6} , which corresponds to 4.6σ in the case of Gaussian errors. Using single-lepton final states, we measure the top quark mass to be 199_{-21}^{+19} (stat.) $_{-21}^{+14}$ (syst.) GeV/c^2 . Using the acceptance calculated at our central top quark mass, we measure the top quark pair production cross section to be $\sigma_{t\bar{t}} = 6.4 \pm 2.2 \text{ pb}$. DØ also sees a hadronic W mass peak ($W \rightarrow jj$) in the $t\bar{t}$ data events. Preliminary results from multivariate analyses and from the $t\bar{t} \rightarrow \text{all-jets}$ channel are discussed. Preliminary determination of the top quark mass using dilepton events yields 145 ± 25 (stat.) ± 20 (syst.) GeV/c^2 .

9. Acknowledgements

I would like to express my appreciation to the organizers of this excellent conference. It is also my pleasure to thank colleagues from DØ who helped me in preparing this article.

DØ thanks the Fermilab Accelerator, Computing, and Research Divisions, and the support staffs at the collaborating institutions for their contributions to the success

of this work. We also acknowledge the support of the U.S. Department of Energy, the U.S. National Science Foundation, the Commissariat à L'Energie Atomique in France, the Ministry for Atomic Energy and the Ministry of Science and Technology Policy in Russia, CNPq in Brazil, the Departments of Atomic Energy and Science and Education in India, Colciencias in Colombia, CONACyT in Mexico, the Ministry of Education, Research Foundation and KOSEF in Korea and the A.P. Sloan Foundation.

10. References

1. P. B. Renton, these Proceedings.
2. DØ Collaboration, S. Abachi *et al.*, Phys. Rev. Lett. **72**, 2138 (1994).
3. CDF Collaboration, F. Abe *et al.*, Phys. Rev. D **50**, 2966 (1994); Phys. Rev. Lett. **73**, 225 (1994).
4. DØ Collaboration, S. Abachi *et al.*, Phys. Rev. Lett. **74**, 2422 (1995).
5. DØ Collaboration, S. Abachi *et al.*, Phys. Rev. Lett. **74**, 2632 (1995).
6. Weiming Yao, these Proceedings;
CDF Collaboration, F. Abe *et al.*, Phys. Rev. Lett. **74**, 2626 (1995).
7. DØ Collaboration, S. Abachi *et al.*, Nucl. Instrum. Methods **A338**, 185 (1994).
8. S. Abachi *et al.*, (DØ Collab.), FERMILAB-PUB-1995/020-E, to be published in Phys. Rev. D.
9. B. Klima (DØ Collab.), FERMILAB-CONF-95-102-E. To be published in the Proceedings of Rencontres de Moriond, Les Arcs, France, Mar. 11-18, 1995.
10. F. Paige and S. Protopopescu, BNL-38034, 1986 (unpublished), v6.49.
11. E. Laenen, J. Smith, and W. van Neerven, Phys. Lett. **321B**, 254 (1994).
12. F. Berends, H. Kuijf, B. Tausk, and W. Giele, Nucl. Phys. **B357**, 32 (1991).
13. F. Carminati *et al.*, "GEANT Guide," CERN Library, 1991 (unpublished).
14. G. Marchesini *et al.*, Comput. Phys. Commun. **67**, 465, (1992).
15. H.E. Miettinen (DØ Collab.), DØ Note # 2527. To be published in the Proceedings of the 4th International Workshop on Artificial Intelligence for High Energy and Nuclear Physics, Pisa, Italy, Apr. 3-8, 1995.
16. P. C. Bhat (DØ Collab.), Proceedings of the 8th meeting of the Division of Particles and Fields of the APS, Vol. 1, p. 705, 1994; FERMILAB-CONF-95-211-E. To be published in the Proceedings of 10th Workshop on $p\bar{p}$ Collider Physics, Fermilab, Batavia, IL, May 9-13, 1995.
17. F. Berends, H. Kuijf, B. Tausk and W. Giele, Nucl. Phys. **B357**, 32 (1991).
18. JETNET 3.0 LUND Preprint, LU TP 93-29 (1993).
19. K. Kondo, Journal of the Physical Society of Japan, vol. 57, no. 12, 4126 (1988) and vol. 60, no. 3, 836 (1991); R. H. Dalitz and G. R. Goldstein, Phys. Rev. D **45**, 1531 (1992) and Oxford preprint OUTP-92-07P.
20. U. Heintz and J. Cochran, DØ note # 2659.